FERMILAB-PUB-22-577-TD (ACCEPTED)
DOI: 10.1016/j.cryogenics.2022.103598

A bi-layer barrier design for 122-type iron-based superconducting wires and tapes

Xingchen Xu*, Fang Wan, Zuhawn Sung

Fermi National Accelerator Laboratory, Batavia, IL 60510, U.S.A

* Corresponding author. E-mail: xxu@fnal.gov

Abstract

Iron-based superconducting wires and tapes hold great promise for high-field magnet applications. A promising design for 122-type wires and tapes based on the powder-in-tube method is using silver and copper double-layer sheaths. For this design a heat treatment temperature below ~779°C is required to prevent Ag-Cu liquid formation. However, this may be below the optimal heat treatment temperature for the critical current density, and still cannot prevent Ag-Cu interdiffusion occurring in the solid state. In this work we propose adding a niobium or tantalum or vanadium (or their alloys) barrier layer between the Ag and Cu to solve the Ag-Cu interdiffusion issue, given that the group-VB metals (vanadium, niobium, tantalum) are relatively inert to both Ag and Cu. To investigate the effectiveness of this design, $BaFe_{1.84}Co_{0.16}As_2$ wires and tapes with Ag/Cu and Ag/Ta/Cu sheaths, as well as $Ba_{0.6}K_{0.4}Fe_2As_2$ wires and tapes with Ag/Cu and Ag/Nb/Cu sheaths, were fabricated. It was found that both the Ta and Nb layers kept integral after wire drawing, but after a large flat-rolling reduction the Ta layer broke while the Nb layer kept integral. In the tapes with Ag/Cu sheaths (without the Ta or Nb layer) Cu diffused through the Ag layer and into the powder cores during 740°C heat treatment, while in the tapes with Ag/Nb/Cu sheaths the Nb layer effectively blocked Ag-Cu interdiffusion even at 900°C. This work demonstrates that Ta is a suitable barrier material for

122-type wires, while Nb is suitable for both wires and tapes. In this design using Ag/Nb (or Ta)/Cu sheaths, we can regard the outer Cu as the conductor matrix while the Ag and Nb (or Ta) serve as two layers of barriers that suppress reactions between the components. Thus, we call this design a "bi-layer barrier" design for 122-type wires and tapes.

Keywords: iron-based superconductors, interdiffusion, sheath materials, heat treatment.

1. Introduction

Iron-based superconductors (IBS), despite their youngness, have shown great promise for high-field magnet applications [1-4]. Among the various types of IBS that can be fabricated into wires and tapes using the powder-in-tube (PIT) method, the 122 family achieves the best current-carrying performance at present [3, 5-7]. The 122-type IBS, with critical temperature (T_c) up to 38 K [8,9], upper critical field above 100 T [10], relatively small anisotropy (~2) [11-13] compared with other high temperature superconductors, have a potential to offer unique advantages over other superconductors. Compared with NbTi and Nb_3Sn, they may be used at higher temperature (e.g., 20 K) and higher field [2,3]. Compared with ReBCO coated conductors, they can be fabricated into multifilamentary, round wires that are more convenient for the construction of many types of magnets [14-17]. Compared with BSCCO wires and tapes, their advantage is the potential for lower cost and higher mechanical strength because they do not have to use only Ag (or Ag-rich alloys) as the matrix. Presently the primary issue limiting their application is the relatively low critical current density (J_c) compared with other superconductors at the relevant fields. The highest reported J_c values at 4.2 K, 10 T presently for IBS wires and tapes are 5.4×10^4 A/cm^2 [14] and 1.5×10^5 A/cm^2 [18], respectively. The flat-rolling process, which turns wires into tapes, strongly enhances J_c by inducing c-axis texture in

the IBS and reducing grain misalignment [18]. As IBS are still in the early stage of development, there is still significant potential for further improvement. Studies in order to better understand the impurity segregation and compositional variations that limit the intergranular J_c [19-21], the factors influencing the grain orientation [22], the flux pinning mechanism in the IBS materials (e.g., [23]), among other aspects, may all contribute to further J_c improvement.

Another factor that significantly impacts the IBS performance is the sheath material. Ag is the metal that has the least reaction with 122 powders [24], so Ag and Ag-rich alloys [25] are usually used to contain 122 powders. However, using only Ag as the matrix would lead to high cost and weak conductor strength as Ag is soft. An alternative design that has become more and more common is using Ag/Cu double-layer sheaths (i.e., an Ag tube encompasses the IBS powder while a Cu tube is outside the Ag tube) [26-28]. Cu is a preferred material for the matrices of superconductors due to its multiple advantages: high electrical and thermal conductivities, good drawability, relatively low cost, being non-magnetic, etc.. However, a problem with this design is the Ag-Cu interdiffusion during heat treatment. At 779°C Ag and Cu even form a liquid. To prevent the liquid formation, heat treatment temperatures below 770°C have usually been used [26-29]. However, even though no liquid forms in this low temperature range, Ag and Cu can still inter-diffuse in the solid state and this is detrimental to the conductor residual resistivity ratio (RRR) and thermal conductivity [30]. Furthermore, previous studies to investigate the effect of heat treatment on the superconducting properties of 122 tapes showed that J_c increased monotonically as the heat treatment temperature was increased from 700 to 800 and further to 850-900°C, due to improved grain connectivity and c-axis texture [31,32]. However, in the Ag/Cu double-sheath design the low temperature required to avoid Ag-Cu liquid formation is significantly below the optimal heat treatment temperature. Thus, a solution to

prevent Ag-Cu interdiffusion and allow a much wider heat treatment temperature window may contribute to further J_c improvement of 122-type wires and tapes.

In order to block Ag-Cu interdiffusion we proposed a new design in 2021 [33], which adds a layer of niobium or tantalum or vanadium (or one of their alloys) between Ag and Cu because the group-VB metals (vanadium, niobium and tantalum) are relatively inert to both Ag and Cu. For example, they are immiscible with Ag, and their solubility in Cu is negligible, while Cu has small solubility (<2 at.%) in V and Nb (but not in Ta) at 900°C [34-36]. This work will explore the feasibility of using Nb or Ta, with the goal of investigating if this Nb or Ta layer can: (1) keep integral during wire drawing and flat-rolling, (2) prevent Ag-Cu interdiffusion for high heat treatment temperatures (e.g., up to 850-900°C that was demonstrated to be the optimal range for J_c [31,32]).

2. Experimental

Two 122-type IBS powders, with nominal compositions of $BaFe_{1.84}Co_{0.16}As_2$ and $Ba_{0.6}K_{0.4}Fe_2As_2$, respectively, were produced at Tokyo University of Agriculture and Technology (TUAT). To prepare the Co-doped 122 powder, Ba, Fe, Co, As with molar ratios of 1:1.84:0.16:2 were mixed and ball milled in Ar atmosphere [37,38]. Then the powder was compressed into a pellet, sealed in a quartz tube under vacuum and sintered at 900°C for 60 hours before ground into powder, which was then filled into an Ag tube with inner diameter (I.D.) of 4 mm and outer diameter (O.D.) of 6 mm. To make the K-doped 122 powder, Ba, K, Fe, As with molar ratios of 0.6:0.47:2:2.1 (excess K and As were added to compensate their loss) were mixed and ball milled in Ar atmosphere, and the ball-milled powder was directly filled into a 4 mm I.D. × 6 mm

O.D. Ag tube. X-ray diffraction (XRD) measurements verified that the majority of the powders were Ba-122 phases, with some Fe and FeAs phases also found.

Then the powder-filled Ag tubes were sealed in Ar-filled plastic bags and sent to Fermilab for wire fabrication. To compare the wires with and without Ta, a half of the Ag tube filled with the Co-doped 122 powder was wrapped tightly by >2 but <3 turns of 140 μm thick pure Ta foil (fully annealed), while the other half was not covered. Then the Ag tube with the Ta foil was inserted into a 9.4 mm I.D. × 12.7 mm O.D. Cu tube. Similarly, a half of the Ag tube filled with the K-doped 122 powder was tightly wrapped by >2 but <3 turns of 130 μm thick pure Nb foil (fully annealed), and then inserted into a 9.4 mm I.D. × 12.7 mm O.D. Cu tube. Then the assemblies were drawn to 1.21 mm diameter in a wire drawing vendor. No breakage occurred during the wire drawing. This allowed us to obtain four wires: the Co-doped Ba-122 wires with Ag/Cu sheaths and Ag/Ta/Cu sheaths, as well as the K-doped Ba-122 wires with Ag/Cu sheaths and Ag/Nb/Cu sheaths, here named "Co-noTa", "Co-Ta", "K-noNb", and "K-Nb", respectively. The four wires were flat-rolled to 0.4 mm thickness (corresponding to 67% thickness reduction) in 4 passes to check the integrity of the Ta and Nb layers after rolling. After finding that the Nb layer kept integral while the Ta layer had broken after 67% rolling reduction, we also rolled the K-Nb wire to 0.33 and 0.2 mm thicknesses in 5 passes and 7 passes, respectively (corresponding to 73% and 84% reductions, respectively). Here these tapes are denoted "Co-noTa-67%", "Co-Ta-67%", "K-noNb-67%", "K-Nb-67%", "K-Nb-73%", "K-Nb-84%", respectively. For each wire and tape straight segments were sealed in quartz tubes under vacuum and heat treated at 740°C for 12 hours. The Co-Ta and K-Nb wires and tapes were also heat treated at 850°C for 2 hours and at 900°C for 0.5 hours to check the effectiveness of the Ta or Nb layer in blocking the Cu-Ag interdiffusion at high temperatures.

Cross sections of the samples were polished for scanning electron microscopy (SEM) and X-ray energy-dispersive spectroscopy (EDS) studies, for which an accelerating voltage of 25 kV was used. The error for the EDS measurements is about 1 at.%, and due to the interaction volume there is a transition width of a few microns for an EDS line scan across an interface. Samples of 3-4 mm lengths were measured in a vibrating sample magnetometer (VSM) for magnetization versus temperature (*M*-*T*) curves at 1 mT, with the sample length perpendicular to the magnetic field. RRR values of some samples were measured using the four-point method at zero field; a sensing current of 1 A was used, and the voltage tap separation was 5 mm. The RRR values were taken as the resistances at room temperature (about 295 K) over those at 40 K, which is above the T_c of the Ba-122 samples.

3. Results and discussions

Fig. 1 shows SEM images of the four wires without heat treatment. Both the Ta and the Nb layers kept integral after wire drawing. It is also seen that the Ta or Nb does not have a uniform layer thickness: e.g., the circled regions in Fig. 1 are thinner than the rest of the layers. This thickness non-uniformity was caused by the fact that we wrapped >2 but <3 turns of Ta or Nb foil around each powder-filled Ag tube – the thinner regions were just the parts that were not covered by the third foil turn. In this work we simply used foils to add the Ta or Nb layer for the demonstration purpose; however, for future production of IBS wires and tapes, use of Ta or Nb tubes is preferred – this should solve the thickness non-uniformity issue and also benefit wire drawing and rolling. It is also seen that the Ta layer has a higher degree of surface roughness than the Nb layer. This is perhaps because the mechanical property mismatch between the hard Ta and the soft Cu (or Ag) is higher than the mismatch between Nb and Cu (or Ag): e.g., both

the yield strength and the work hardening rate of Ta are much higher than those of Cu [39]. Higher surface roughness is certainly undesirable because it may make the layer easier to break. On the other hand, given that Ta has been used successfully for decades as the standard barrier material for bronze-process and single-barrier internal-tin Nb_3Sn wires even with large drawing strains [40], we believe that Ta can also be a suitable barrier material for 122 wires, provided that large flat-rolling reduction is not required (as discussed below).

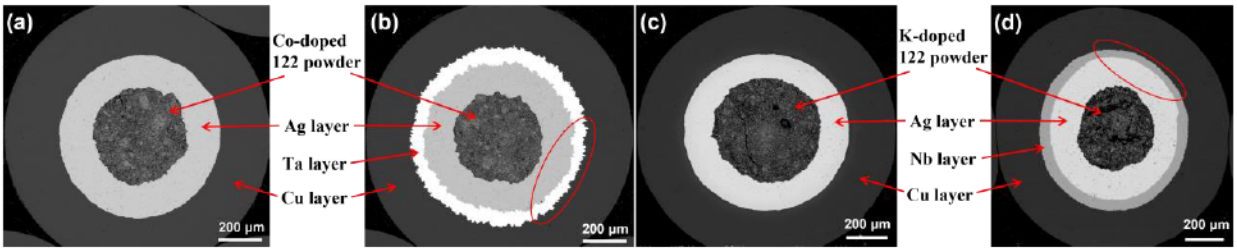

Fig. 1. SEM images of (a) Co-noTa, (b) Co-Ta, (c) K-noNb, (d) K-Nb wires without heat treatment. The circled regions are thinner than the rest of the Ta and Nb layers.

Fig. 2 shows SEM images of all of the tapes before heat treatment. It is seen from Fig. 2b that some gaps emerge in the Ta layer, indicating that it broke during flat-rolling. In contrast, no opening was found in the Nb layer in any of the K-Nb tapes (for each tape multiple cross sections were observed), indicating that the Nb layer kept integral during flat-rolling, even for a reduction as high as 84%. The reason why Ta could not perform as well as Nb during flat-rolling is perhaps related to its higher yield strength and the higher surface roughness mentioned above (the layer tends to break at the indentations, especially as the layer becomes thin).

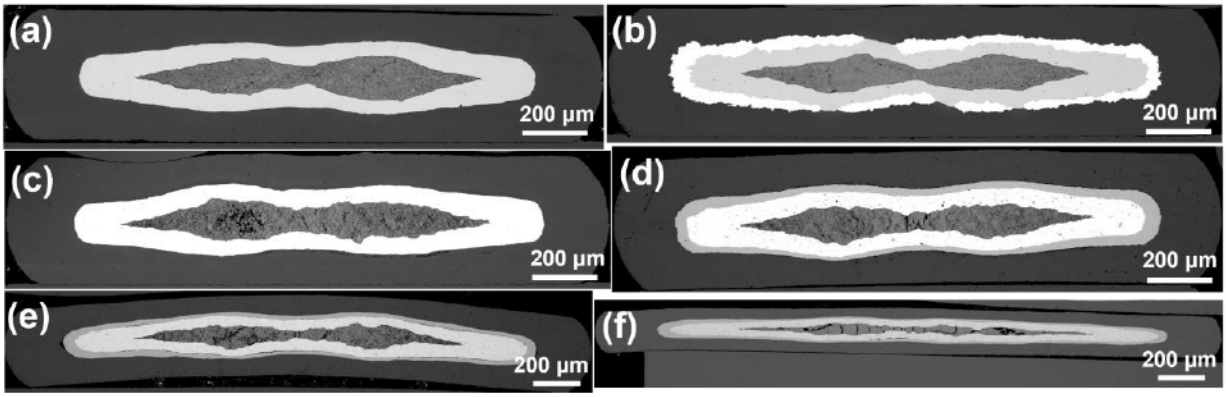

Fig. 2. SEM images of (a) Co-noTa-67%, (b) Co-Ta-67%, (c) K-noNb-67%, (d) K-Nb-67%, (e) K-Nb-73%, and (f) K-Nb-84% tapes before heat treatment.

Fig. 3 shows SEM images of the Co-Ta-67% tape and the K-Nb-84% tape after the 850°C/2h heat treatment as well as the K-Nb-84% tape after the 900°C/0.5h heat treatment. As a result of the Ta layer breakage, Ag-Cu interdiffusion occurred through the gaps in the Ta layer in the Co-Ta-67% tape, forming Ag-Cu liquid (Fig. 3a). On the other hand, the integral Nb layer prevented liquid formation in the K-Nb-84% tapes for both the 850°C and 900°C heat treatments. However, we did observe a few tiny, localized leakage spots (much smaller than 1 mm) at one of the two faces of the K-Nb-84%-850°C/2h tape (but not at the K-Nb-67% or the K-Nb-73% tapes heat treated at 850°C or 900°C), indicating that the Nb layer was discontinuous at a few tiny spots in the K-Nb-84% tape. This is most likely due to the thickness non-uniformity of the Nb layer – i.e., the thin region (circled in Fig. 1d) was not thick enough to keep integral everywhere after 84% rolling reduction, which explains why only one face of the K-Nb-84%-850°C/2h tape had such leakage spots while the other face did not. Thus, we believe that this problem can be solved if a uniform Nb layer (e.g., by using Nb tubes instead of foils) with a thickness above the "safety threshold" is used. It is worth mentioning that this is also related to the flat-rolling

process: we tried flat-rolling the K-Nb wire to 0.2 mm thickness in one pass but saw a severe leakage after 850°C heat treatment, indicating that the rolling technique has a critical influence on the Nb layer.

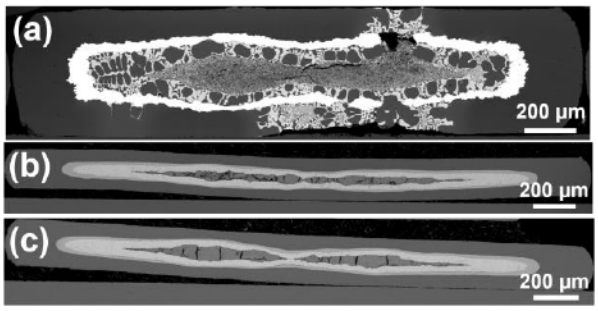

Fig. 3. SEM images of (a) the Co-Ta-67% and (b) the K-Nb-84% tapes after 850°C/2h heat treatment, and (c) the K-Nb-84% tape after 900°C/0.5h heat treatment.

To further verify if any reactions between the components occurred, the elemental distributions in these tapes were measured. EDS line scans starting from the powder core region and ending within the outer Cu region were obtained for the Co-noTa-67% and the K-noNb-67% tapes after the 740°C/12h heat treatment and are shown in Fig. 4.

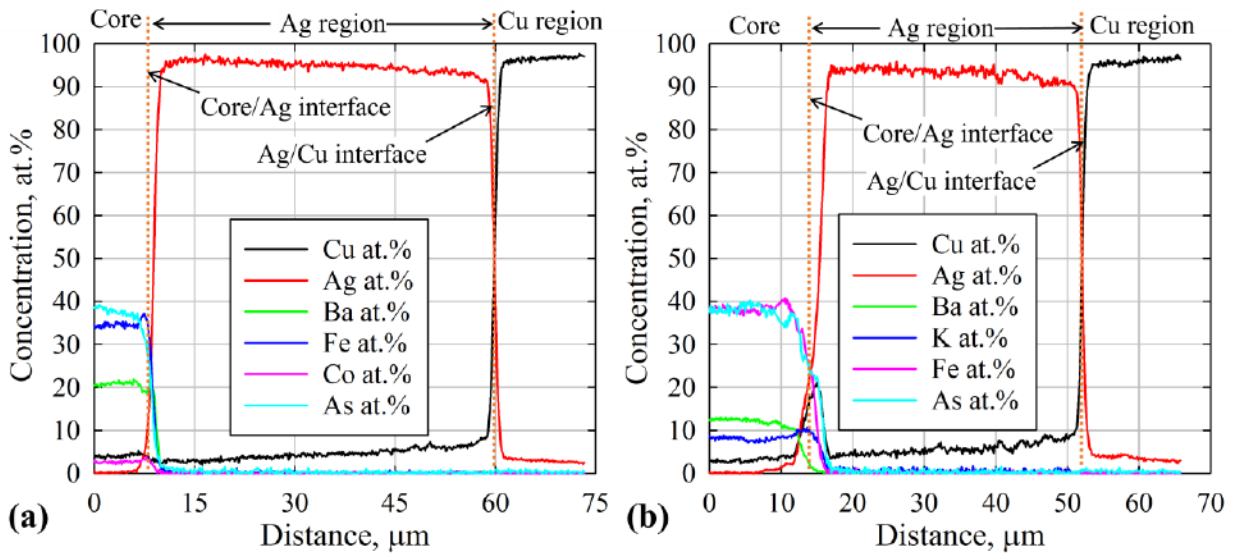

Fig. 4. EDS line scans starting from the powder core region and ending within the outer Cu region for (a) the Co-noTa-67% and (b) the K-noNb-67% tapes after the 740°C/12h heat treatment.

From Fig. 4 it is seen that the Co-noTa-67% and the K-noNb-67% tapes show similar phenomena. (1) Ag diffused into the outer Cu, forming a Cu-Ag solid solution with Ag content as high as 4at.%. This would inevitably reduce the matrix RRR and thermal conductivity [30]. (2) Cu diffused into Ag, and the Cu content in the Ag-Cu solid solution was as high as 9at.%. Notably, Cu diffused across the whole Ag layer. (3) Cu also diffused into the IBS core, with a content as high as 5at.%. How Cu distributes in the IBS powder (e.g., at grain boundaries or in the lattice) and how it affects the IBS J_c still requires further studies. The diffusion of Cu across the Ag layer and into the IBS core is driven by the gradient of the chemical potential of Cu. Of course, this can be suppressed by increasing the Ag layer thickness or reducing the heat treatment temperature or time, but the former would lead to increased conductor cost and

reduced strength, while the latter may reduce J_c if the heat treatment is lighter than the optimal schedule.

An EDS line scan was also obtained for the K-Nb-84% tape after the 850°C/2h heat treatment and is shown in Fig. 5. It can be seen that Ag did not diffuse into the Cu layer. The measured RRR (the ratio of the resistivity at 295 K to that at 40 K) of the K-Nb-84%-850°C/2h tape was 32, noticeably higher than those of the Co-noTa-67% and K-noNb-67% tapes after 740°C/12h heat treatment (20 and 17, respectively). Although some Cu diffused into the Nb perhaps because Cu has a little solubility in Nb (< 2 at.% at 900°C) [35], the Cu content in the Ag layer was very low and that in the IBS core was negligible, indicating that the Nb layer effectively blocked Ag-Cu interdiffusion. On the other hand, an As peak is seen at the Ag/Nb interface. We indeed found an As-containing layer (<1 μm thick) at the Ag/Nb interface, but our EDS measurements of the cores showed that it had little influence on the IBS powder composition. The average composition of the IBS cores of the K-Nb tapes was 12.2at.%Ba, 8.9at.%K, 40.3at.%Fe, 38.6at.%As, while that of the K-noNb tapes was 12.1at.%Ba, 8.8at.%K, 40.5at.%Fe, 38.6at.%As. Thus, we do not expect this to affect the IBS superconducting properties. The cause for the presence of As in the Ag/Nb interface is worth further investigation. It is worth mentioning that our EDS measurements on the Co-Ta wire after the 850°C/2h heat treatment (which had no Cu-Ag liquid formation at all due to the intact Ta barrier layer) showed that no Cu diffused into the Ta layer or the Ag layer (probably due to the fact that Cu and Ta have no solubility in each other [36]) and that there was no As in the Ag/Ta interface. This indicates that for 122-type wires, Ta may be a better barrier material than Nb.

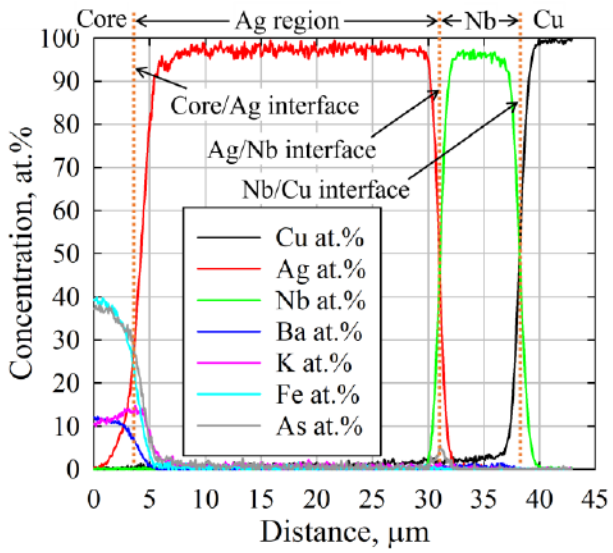

Fig. 5. EDS line scan starting from the powder core region and ending within the outer Cu region for the K-Nb-84% tape after the 850°C/2h heat treatment.

We also attempted to measure the superconducting properties of these samples. However, the *M-T* curves showed broad T_c transitions and relatively large variations along the sample length for all of the samples (both the Co-doped and K-doped wires or tapes), indicating that there was certain degree of inhomogeneity in our 122 powders. This makes a fair comparison between the samples with different designs impossible. As this was our first trial in fabricating 122 wires, some problems might have occurred during fabrication of the powders or wires (for example, the lack of the pre-sintering step for the K-doped powder may be a cause of the problem). On the other hand, this does not affect the completeness of this study because its major purpose is to investigate if this new design can solve the Ag-Cu interdiffusion issue in a wide temperature range. From this perspective the conclusion is already quite clear from the above metallography and composition results, which demonstrate that addition of an Nb layer (or a Ta layer for wires) with a uniform thickness above the safety threshold can indeed prevent Ag-Cu interdiffusion or

liquid formation at high temperatures. Using this design to fabricate 122-type wires and tapes to achieve high performance, which requires high-quality and uniform 122 powders, will be pursued in subsequent efforts and also possibly by other groups. We hope that this new design, by allowing the use of the optimal heat treatment, can contribute to further J_c improvement for 122-type wires and tapes. Another interesting question to be investigated is, whether the lower thermal expansion of Nb (or Ta if to be used in a round wire) and its higher strength at high temperatures may help in constraining the IBS core expansion during heat treatment, leading to densification of IBS core and benefiting J_c.

Finally, it is worth mentioning that in this new design, the Cu can be the major component for the conductor matrix while the Ag and the Nb (or Ta) layers can be much thinner than Cu, provided that they keep intact everywhere after the mechanical deformations (e.g., wire drawing and rolling). If we compare the IBS with this design to the widely-used NbTi and Nb_3Sn conductors, we can still regard the Cu as the matrix, and regard the Ag and Nb (or Ta) layers as two additional barriers to overcome the chemical incompatibility between the components: the function of the Ag layer is to prevent reaction between the 122 powder and the Nb (or Ta) layer, while the function of the Nb (or Ta) layer is to prevent Ag-Cu interdiffusion. Thus, we refer to this design as "bi-layer barrier" design for 122 PIT wires and tapes. This design can be used for both mono-filamentary and multi-filamentary wires and tapes.

4. Conclusions

This work proposes a bi-layer barrier design for 122-type wires and tapes, in which Cu is the major matrix while Ag and Nb (or Ta) layers serve as two chemical barriers to prevent reactions between components during heat treatment. To investigate the effectiveness of this design, Ba-

122 wires and tapes with and without a Ta or Nb layer were fabricated. It turned out that both the Ta and the Nb layers kept integral after wire drawing, but Ta broke during flat-rolling, while the Nb layer kept intact even for large rolling reductions. This demonstrates that Nb is a suitable barrier material for both wires and tapes, while Ta is usable for wires. Composition studies showed that for the tapes with Ag/Cu sheaths (i.e., without the Ta or Nb barrier), Cu diffused across the Ag layer and into the IBS core, while an intact Nb barrier could effectively prevent Ag-Cu interdiffusion and prevent Cu diffusing into IBS core even at 900°C. We propose to use this bi-layer barrier design for further improvement of IBS wires and tapes performance.

CRediT authorship contribution statement

Xingchen Xu: Conceptualization, Methodology, Investigation, Formal analysis, Writing – original draft. **Fang Wan:** Investigation, Formal analysis. **Zuhawn Sung:** Funding acquisition.

Acknowledgement

This work is supported by a Lab-Directed R&D (LDRD) project in Fermilab. This manuscript has been produced by Fermi Research Alliance, LLC under Contract No. DE-AC02-07CH11359 with the U.S. Department of Energy, Office of Science, Office of High Energy Physics. The authors thank Yuta Hasegawa, Shinjiro Kikuchi, and Akiyasu Yamamoto of Tokyo University of Agriculture and Technology (TUAT) for providing the two 122-type IBS powders.

References

[1]. Kamihara Y, Watanabe T, Hirano M, Hosono H. Iron-based layered superconductor La[O_{1-x} F_x]FeAs (x = 0.05-0.12) with T_c = 26 K. J Am Chem Soc 2008;130:3296-7.
[2]. Hosono H, Yamamoto A, Hiramatsu H, Ma YW. Recent advances in iron-based superconductors toward applications. Mater Today 2018;21:278-302.
[3]. Yao C, Ma Y. Recent breakthrough development in iron-based superconducting wires for practical applications. Supercond Sci Technol 2019;32:023002.
[4]. Zhang Z, Wang DL, Wei SQ, Wang YZ, Wang CT, Zhang Z, Yao HL, Zhang XP, Liu F, Liu HJ, Ma YW, Xu QJ, Wang YF. First performance test of the iron-based superconducting racetrack coils at 10 T. Supercond Sci Technol 2021;34:035021.
[5]. Zhang X P, Yao C, Lin H, Cai Y, Chen Z, Li JQ, Dong CH, Zhang QJ, Wang DL, Ma YW, Oguro H, Awaji S, Watanabe K. Realization of practical level current densities in $Sr_{0.6}K_{0.4}Fe_2As_2$ tape conductors for high-field applications. Appl Phys Lett 2014;104:202601.
[6]. Pyon S, Miyawaki D, Tamegai T, Awaji S, Kito H, Ishida S, Yoshida Y. Enhancement of critical current density in (Ba,Na)Fe_2As_2 round wires using high-pressure sintering. Supercond Sci Technol 2020;33:065001.
[7]. Jin ZK, Liu C, Yao C, Li L, Huang H, Wang DL, Dong CH, Wang K, Zhang XP, Awaji S, Ma YW. Properties of seven-filament Cu/Ag-sheathed (Ba,K)Fe_2As_2 tapes fabricated from round and square wires. Rare Met 2020;40:3651-9.
[8]. Rotter M, Tegel M, Johrendt D. Superconductivity at 38 K in the iron arsenide ($Ba_{1-x}K_x$)Fe_2As_2. Phys Rev Lett 2008;101:107006.
[9]. Sasmal K, Lv B, Lorenz B, Guloy AM, Chen F, Xue YY, Chu CW. Superconducting Fe-based compounds ($A_{1-x}Sr_x$)Fe_2As_2 with A = K and Cs with transition temperatures up to 37 K. Phys Rev Lett 2008;101:107007.
[10]. Ni N, Budko SL, Kreyssig A, Nandi S, Rustan GE, Goldman AI, Gupta S, Corbett JD, Kracher A, Canfield PC. Anisotropic thermodynamic and transport properties of single-crystalline $Ba_{1-x}K_xFe_2As_2$ (x = 0 and 0.45). Phys Rev B 2008;78:014507.
[11]. Yuan HQ, Singleton J, Balakirev FF. Nearly isotropic superconductivity in (Ba,K)Fe_2As_2. Nature 2009;457:565–8.
[12]. Altarawneh MM, Collar K, Mielke CH, Ni N, Bud'ko SL, Canfield PC. Determination of anisotropic H_{c2} up to 60 T in $Ba_{0.55}K_{0.45}Fe_2As_2$ single crystals. Phys Rev B 2008;78: 220505(R).
[13]. Wang XL et al. Very strong intrinsic flux pinning and vortex avalanches in (Ba,K)Fe_2As_2 superconducting single crystals. Phys Rev B 2010;82:024525.
[14]. Pyon S, Mori H, Tamegai T, Awaji S, Kito H, Ishida S, Yoshida Y, Kajitani H, Koizumi N, Fabrication of small superconducting coils using (Ba,A)Fe_2As_2 (A: Na, K) round wires with large critical current densities. Supercond Sci Technol 2021;34:105008.
[15]. Liu SF, Yao C, Huang H, Dong CH, Guo WW, Cheng Z, Zhu YC, Awaji S, Ma YW. Enhancing transport performance in 7-filamentary $Ba_{0.6}K_{0.4}Fe_2As_2$ wires and tapes via hot isostatic pressing. Physica C 2021;585:1353870.
[16]. Miyawaki D, Pyon S, Suwa T, Takano K, Kajitani H, Koizumi N, Awaji S, Tamegai T. Fabrications and evaluations of critical current density of (Ba,Na)Fe_2As_2 HIP round wires. Physica C 2020;568:1353580.
[17]. Guo WW, Yao C, Huang H, Dong CH, Liu SF, Wang CD, Ma YW. Enhancement of transport J_c in (Ba,K)Fe_2As_2 HIP processed round wires. Supercond Sci Technol 2021;34:004001.

[18]. Huang H, Yao C, Dong CH, Zhang XP, Wang DL, Cheng Z, Li J, Awaji S, Wen HH, Ma YW. High transport current superconductivity in powder-in-tube $Ba_{0.6}K_{0.4}Fe_2As_2$ tapes at 27 T. Supercond Sci Technol 2018;31:015017.
[19]. Kim YJ, Weiss JD, Hellstrom EE, Larbalestier DC, Seidman DN. Evidence for composition variations and impurity segregation at grain boundaries in high current-density polycrystalline K- and Co-doped $BaFe_2As_2$ superconductors. Appl Phys Lett 2014;105:162604.
[20]. Kametani F, Su YF, Collantes Y, Pak C, Tarantini C, Larbalestier D, Hellstrom E. Chemically degraded grain boundaries in fine-grain $Ba_{0.6}K_{0.4}Fe_2As_2$ polycrystalline bulks. Appl Phys Express 2020;13:113002.
[21]. Pak C, Su YF, Collantes Y, Tarantini C, Hellstrom EE, Larbalestier DC, Kametani F. Synthesis routes to eliminate oxide impurity segregation and their influence on intergrain connectivity in K-doped $BaFe_2As_2$ polycrystalline bulks. Supercond Sci Technol 2020;33:084010.
[22]. Huang H, Yao C, Dong CH, Zhang XP, Wang DL, Liu S, Cheng Z, Zhu YC, Ma YW. Visualization of the grain structure in high performance $Ba_{1-x}K_xFe_2As_2$ superconducting tapes. Supercond Sci Technol 2021;34:045017.
[23]. Dong CH, Huang H, Ma YW. Slow vortex creep induced by strong grain boundary pinning in advanced Ba122 superconducting tapes. Chinese Phys Lett 2019;36:067401.
[24]. Wang L, Qi YP, Wang DL, Zhang XP, Gao ZS, Zhang ZY, Ma YW, Awaji S, Nishijima G, Watanabe K. Large transport critical currents of powder-in-tube $Sr_{0.6}K_{0.4}Fe_2As_2$/Ag superconducting wires and tapes. Physica C 2010;470:183-6.
[25]. Togano K, Gao Z, Matsumoto A, Kikuchi A, Kumakura H. Fabrication of $(Ba,K)Fe_2As_2$ tapes by *ex situ* PIT process using Ag-Sn alloy single sheath. Supercond Sci Technol 2017;30:015012.
[26]. Weiss JD, Tarantini C, Jiang J, Kametani F, Polyanskii AA, Larbalestier DC, Hellstrom EE. High intergrain critical current density in fine-grain $(Ba_{0.6}K_{0.4})Fe_2As_2$ wires and bulks. Nat Mater 2012;11:682-5.
[27]. Pyon S, Suwa T, Park A, Kajitani H, Koizumi N, Tsuchiya Y, Awaji S, Watanabe K, Tamegai T. Enhancement of critical current densities in $(Ba,K)Fe_2As_2$ wires and tapes using HIP technique. Supercond Sci Technol 2016;29:115002.
[28]. Liu SF, Lin KL, Yao C, Zhang XP, Dong CH, Wang DL, Awaji S, Kumakura H, Ma YW. Transport current density at temperatures up to 25 K of Cu/Ag composite sheathed 122-type tapes and wires. Supercond Sci Technol 2017;30:115007.
[29]. Pyon S, Tamegai T, Takano K, Kajitani H, Koizumi N, Awaji S. Recent progress of iron-based superconducting round wires. J Phys: Conf Ser 2019;1293:012042.
[30]. Dong CH, Zhu YC, Liu SF, Zhang XP, Cheng Z, Huang H, Yao C, Wang DL, Ma YW. Thermal conductivity of composite multi-filamentary iron-based superconducting tapes. Supercond Sci Technol 2022;33:075010.
[31]. Lin H, Yao C, Zhang XP, Dong CH, Zhang HT, Wang DL, Zhang QJ, Ma YW, Awaji S, Watanabe K, Tian HF, Li JQ. Hot pressing to enhance the transport J_c of $Sr_{0.6}K_{0.4}Fe_2As_2$ superconducting tapes. Sci Rep 2014;4:6944.
[32]. Huang H, Yao C, Li L, Dong CH, Liu SF, Zhang XP, Zhu YC, Cheng Z, Ma YW. Effects of heat treatment temperature on the superconducting properties of $Ba_{1-x}K_xFe_2As_2$ tapes. Supercond Sci Technol 2019;32:025007.

[33]. Xu X, Iron-based superconductors with bi-layer barriers. Fermilab Invention Disclosure, submitted in August 2021
[34]. Okamoto H. Cu-V (Copper-Vanadium). J Phase Equilib Diffus 2010;31:83–4. https://doi.org/10.1007/s11669-009-9631-x
[35]. Okamoto H. Cu-Nb (Copper-Niobium). J Phase Equilib Diffus 2012;33:344. https://doi.org/10.1007/s11669-012-0051-y
[36]. Subramanian PR, Laughlin DE. The Cu-Ta (Copper-Tantalum) system. Bulletin of Alloy Phase Diagrams 1989;10:652-5. https://doi.org/10.1007/BF02877637
[37]. Tokuta S, Yamamoto A. Enhanced upper critical field in Co-doped Ba122 superconductors by lattice defect tuning. APL Mater 2019;7:111107.
[38]. Tokuta S, Yamamoto A. Thermal response of the iron-based Ba122 superconductor to in situ and *ex situ* processes. Supercond Sci Technol 2021;34:034004.
[39]. Hartwig KT, Balachandran S, Mathaudhu SN, Barber RE, Pyon T, Griffin RB. Interface Roughness in Copper-Tantalum Wire and Nb_3Sn Superconductor Composites. AIP Conf Proc 2008;986:325-32.
[40]. Xu X. A review and prospects for Nb_3Sn superconductor development. Supercond Sci Technol 2017;30:093001.